# Use of the Teager-Kaiser energy operator for condition monitoring of a wind turbine gearbox

**I. Antoniadou** [1], **G. Manson** [1], **N. Dervilis** [1], **T. Barszcz** [2], **W.J. Staszewski** [2], **K. Worden** [1]
[1] Dynamics Research Group, Mechanical Engineering Department, The University of Sheffield,
Mappin Street, Sheffield S1 3JD, UK
e-mail: **I.Antoniadou@sheffield.ac.uk**

[2] Department of Robotics and Mechatronics, Faculty of Mechanical Engineering and Robotics, AGH University of Science and Technology,
Al. Mickiewicza 30, 30-059 Krakow, Poland

## Abstract
This paper deals with the condition monitoring of a wind turbine gearbox under varying operating conditions, which cause nonstationarity. The gearbox vibration signals are decomposed into a set of monocomponent signals using the Empirical Mode Decomposition (EMD) method. The Teager-Kaiser Energy Operator (TKEO) in combination with an energy separation method is also presented as an alternative technique that seems to improve the time-frequency analysis of signals. In this study, the TKEO is applied to the signal components who's frequency bandwidth is related to the frequencies more influenced by damage. The Teager-Kaiser energy operator is a nonlinear operator that calculates the energy of monocomponent signals as the product of the square of the amplitude and the frequency of the signal. The instantaneous characteristics of these signals are then obtained by the application of the Discrete Energy Separation Algorithm (DESA-2). It will be shown that TKEO improves the estimation of instantaneous characteristics of the vibration data compared to other commonly used techniques, e.g. the Hilbert Transform.

## 1 Introduction

The condition monitoring of wind turbine gearboxes is a necessary practice in order to reduce the costs of corrective maintenance of wind turbine systems. Among other methods, vibration analysis is commonly used for this purpose, and this is based on the idea that the rotating machinery have a specific vibration signature for their standard condition that changes with the development of damage.

Several scientific fields, such as signal processing, statistics and neural networks have been used for structural health monitoring in general and condition monitoring more particularly. A review of such methods was written by Doebling et al.[1]. In the early studies, some of the conventional techniques used were the probability distribution characteristics of the vibration signals such as skewness and kurtosis [2], Fourier analysis and modulation sidebands [3] [4], and Cepstrum analysis [5]. However, as research in the signal processing area developed, the drawback of the assumption of stationarity and linearity of the vibration signals by these methods became more evident. To deal with nonstationary signals, attention was given to time-frequency analysis methods such as the Wigner-Ville distribution [6], wavelet analysis [7], cyclostationary analysis [8] and spectral correlation. Wavelet analysis is probably the most popular technique [9], but has the drawback that the basis functions of the decompositions are fixed and do not necessarily match the varying nature of the signals. Relatively recently, in the quest for accurate time and frequency resolution, Huang et al. [10] proposed the Empirical Mode Decomposition method (EMD). Since then, attention was gained in applying the EMD in the damage detection of gears [11, 12]. The EMD technique decomposes the signal into intrinsic

mode functions and the instantaneous frequency and amplitude of each intrinsic mode function can be then obtained, most commonly by applying the Hilbert Transform. An alternative approach in order to obtain the instantaneous characteristics of the vibration decomposed signals, is to use an energy tracking operator to estimate the energy of the signal, as developed by Teager [13, 14] and introduced by Kaiser [15, 16], and then use an energy separation algorithm for the estimation of the amplitude envelope and instantaneous frequency of each intrinsic mode function (IMF) produced by the EMD method. The above mentioned method promises high resolution and low computational power compared to other widely used time-frequency techniques.

## 2 The Empirical mode decomposition method

In order to isolate the frequencies of interest when analysing a signal, bandpass filtering is needed. In this way one can exclude parts of the vibration signal not associated with the particular component examined, in this case the gearbox.

The Empirical Mode Decomposition method (EMD) is an empirical method used to decompose a multicomponent signal into a number of signal components (set of oscillatory functions) in the time-domain called intrinsic mode functions (IMF). Each IMF represents a bandwidth of frequencies of the signal, so the EMD method is a filter bank method, and can be used for removing unwanted components of the signal being analysed.

By definition, an IMF should satisfy the following conditions [10]: (a) the number of extrema and the number of zero crossings over the entire length of the IMF must be equal or differ at most by one, and (b) at any point, the mean value of the envelope defined by the local maxima and the envelope defined by the local minima is zero. The EMD decomposition procedure for extracting an IMF is called the *sifting process* and consists of the following steps:

1. The local extrema and the local minima of the signal $x(t)$ are found.
2. All the local extrema of the signal are connected to form the upper envelope $u(t)$, and all the local minima of the envelope are connected to form the lower envelope $l(t)$. This connection is made using a cubic spline interpolation scheme.
3. The mean value $m_1(t)$ is defined as:

$$m_1(t) = \frac{l(t) + u(t)}{2} \tag{1}$$

and the first possible component $h_1(t)$ is given by the equation:

$$h_1(t) = x(t) - m_1(t) \tag{2}$$

The component $h_1(t)$ is accepted as the first component only if it satisfies the conditions to be an IMF. If it is not an IMF, the *sifting process* is followed until $h_1(t)$ satisfies the conditions to be an IMF. During this process $h_1(t)$ is treated as the new data set, which means that its upper and lower envelopes are formed and the mean value of these envelopes, $m_{11}(t)$, is used to calculate a new component $h_{11}(t)$ hoping that it satisfies the IMF criteria:

$$h_{11}(t) = x(t) - m_{11}(t) \tag{3}$$

The *sifting process* is repeated until the component $h_{1k}(t)$ is accepted as an IMF of the signal $x(t)$ and is denoted by $C_1(t)$:

$$C_1(t) = h_{1k}(t) = h_{1(k-1)}(t) - m_{1k}(t) \tag{4}$$

4. The first IMF is subtracted from the signal $x(t)$ resulting in the residual signal:

$$r_1(t) = x(t) - C_1(t) \tag{5}$$

During the *sifting process* the signal $x(t)$ is decomposed into a finite number $N$ of intrinsic mode functions and as a result $N$ residual signals are obtained. The process ends when the last residual signal, $r_N(t)$ is obtained and is a constant or a monotonic function. The original signal $x(t)$ can be reconstructed as the sum:

$$x(t) = \sum_{j=1}^{N} C_j(t) + r_N(t) \tag{6}$$

The nonstationary signal is decomposed into IMFs using the previously described EMD algorithm. Each IMF can be then analysed separately in order to obtain features for damage detection.

## 3 The Hilbert Transform

In order to estimate the instantaneous frequency and instantaneous amplitude of a signal a standard approach is to use the Hilbert Transform (HT). So after decomposing the signal into IMFs using the EMD algorithm, one can use the Hilbert transform to derive the analytic signal. If $\hat{x}(t)$ is the HT of a signal $x(t)$, it is given by the equation:

$$\hat{x}(t) = \frac{1}{\pi} \int_{-\infty}^{+\infty} \frac{x(z)}{t-z}\,\mathrm{d}z = x(t) * \frac{1}{\pi t} \tag{7}$$

Given $\hat{x}(t)$ one can define the analytic signal, introduced by [17]:

$$z(t) = x(t) + i\hat{x}(t) \tag{8}$$

where $i$ is the imaginary unit.

The above equation written in its exponential form gives:

$$z(t) = A(t)e^{i\phi(t)} \tag{9}$$

where $A(t)$ is the amplitude envelope of the signal, and $\phi(t)$ the instantaneous phase.

The amplitude envelope and instantaneous phase can be estimated by the following equations:

$$A(t) = \sqrt{x(t)^2 + \hat{x}(t)^2} = |z(t)| \tag{10}$$

$$\phi(t) = arctan(\hat{x}(t)/x(t)) = Arg(z(t)) \tag{11}$$

and the instantaneous frequency can be calculated by:

$$\omega(t) = \frac{1}{\pi}\frac{d\phi(t)}{dt} \tag{12}$$

Combining the above with the EMD method, the original signal $x(t)$ can be expressed as:

$$x(t) = Re\{\sum_{j=1}^{N} A_j(t)e^{i\int \omega_j(t)dt}\} \tag{13}$$

where $j$ is the number of the IMFs and $A_j$ and $\omega_j$ the instantaneous amplitude and instantaneous frequency of the $j^{th}$ IMF. The above equation enables one to represent the instantaneous amplitude and instantaneous frequency of the signal in a three-dimensional plot. This time-frequency representation is designated as the Hilbert spectrum.

## 4 Teager-Kaiser energy operator

The energy of a signal $x(t)$ is given by the equation:

$$E = \int_{-T}^{T} |x(t)|^2 \mathrm{dt} \tag{14}$$

This is not the instantaneous summed energy but the energy of the signal over a time $2T$. Another way to estimate a signal's energy, is to use the squared absolute value of the different frequency bands of the Fourier transformed signal as a measure of the energy levels of respective bands. What Kaiser observed, by studying a second order differential equation, is that the energy to generate a simple sinusoidal signal varies with both amplitude and frequency. Finally, in order to estimate the instantaneous energy of a signal is using an energy tracking operator. This is the so called Teager-Kaiser Energy Operator (TKEO), $\Psi[.]$, and is defined as:

$$\Psi_c[x(t)] = [\dot{x}(t)]^2 - x(t)\ddot{x}(t) \tag{15}$$

where x(t) is the signal and $\dot{x}(t)$ and $\ddot{x}(t)$ are its first and second derivatives respectively. In the discrete case, the time derivatives of the equation $(15)$ can be approximated by time differences:

$$\Psi_d[x(n)] = x_n^2 - x_{n+1}x_{n-1} \tag{16}$$

The TKEO offers excellent time resolution because only three samples are required for the energy computation at each time instant. The operators $\Psi_c$ and $\Psi_d$ were developed by Teager during his work on speech production modelling [13, 14] where he described the nonlinearities of speech production and showed a plot of the energy creating sound, without giving though the algorithm to calculate this energy. Later, Kaiser presented the algorithm developed by Teager in his work [15, 16]. When $\Psi_c$ is applied to signals produced by a simple harmonic oscillator, e.g. a mass spring oscillator who's equation of motion can be derived from the Newton's Law:

$$\frac{d^2x}{dt^2} + \frac{k}{m}x = 0 \tag{17}$$

It can track the oscillator's energy (per half unit mass) which is equal to:

$$E = \frac{1}{2}kx^2 + \frac{1}{2}m\frac{dx^2}{dt} = \frac{1}{2}m\omega^2A^2 \tag{18}$$

From the above it is obvious that the energy of an object is proportional to $A^2$ and $\omega^2$. Inserting the solution of the equation of motion $(17)$, $x(t) = Acos(\omega t)$, into the equation describing the continuous case of the TKEO $(15)$, it is shown that:

$$\Psi(x(t)) = (-A\omega sin(\omega t))^2 - Acos(\omega t)(-\omega^2 Acos(\omega t)) = A^2\omega^2(sin^2(\omega t) + cos^2(\omega t)) = A^2\omega^2 \quad (19)$$

Therefore, $\Psi_c$ and $\Psi_d$ are energy operators and as a demodulation approach they offer the advantages of high resolution, simplicity and efficiency [20].

# 5 Energy separation algorithm

An alternative approach to that of Hilbert transform separation algorithm application for the estimation of instantaneous envelope $A(t)$ and instantaneous frequency of the signal $\phi(t)$, was developed by [20] and uses an energy tracking operator to estimate initially the required energy for generating the signal being analysed and then to separate it into its amplitude and frequency component using an energy separation algorithm.

If one computes the Teager Energy of a differentiated input signal:

$$\Psi(\dot{x}(t)) = \Psi(-A\omega sin(\omega t)) = A^2\omega^4 cos^2(\omega t) - [-A\omega sin(\omega t)][A\omega^3 sin(\omega t)] = A^2\omega^4 \quad (20)$$

Combining the equation above with the equation $(19)$ one can calculate the frequency and amplitude of the signal $x(t)$:

$$\omega = \frac{1}{2\pi}\sqrt{\frac{\Psi[\dot{x}(t)]}{\Psi[x(t)]}} \quad (21)$$

$$|A(t)| = \frac{\Psi[x(t)]}{\sqrt{\Psi[x(t)]}} \quad (22)$$

These equations estimate exactly the instantaneous frequency and amplitude envelope of a sinusoidal signal, and the approximation errors for the cases of AM, FM and AM-FM signals are small [19].

Two discrete time energy separation algorithms were developed in [20], called DESA-1 and DESA-2. They both produce accurate estimates , by computing the energy operator of the signal and its derivative. The difference consists in the way the derivative is approximated in the discrete-time domain, with DESA-2 having a slight computational advantage.

The DESA-2 algorithm estimates the instantaneous frequency and amplitude using the following equations:

$$\frac{2\Psi_d[x_n]}{\sqrt{\Psi_d[x_{n+1} - x_{n-1}]}} \approx |A(n)| \quad (23)$$

$$\frac{1}{2}arcos(1 - \frac{\Psi_d[x_{n+1} - x_{n-1}]}{2\Psi_d[x_n]}) \approx \Omega_i(n) \quad (24)$$

where:

$$\Omega_i = \omega_i T \quad (25)$$

From equation $(24)$ it can be seen that the frequency of the signal can be uniquely estimated only upto $\frac{\pi}{2}$ (one quarter of the sampling frequency). The frequency $\Omega_i$ of a signal beyond $\frac{\pi}{2}$ is identified as its mirror frequency with respect to $\frac{\pi}{2}$.

## 6 A simulated example

In order to compare the above mentioned methods a simulated example will be first given. A chirp signal was simulated with $10kHz$ sampling rate as shown in Figure 1. The instantaneous frequency and amplitude envelope of the signal were then calculated using both the Hilbert Transform and the TKEO in combination with an the energy separation algorithm DESA-2. It is obvious from the figures that for high sampling frequencies the TKEO with DESA-2 method improves the results.

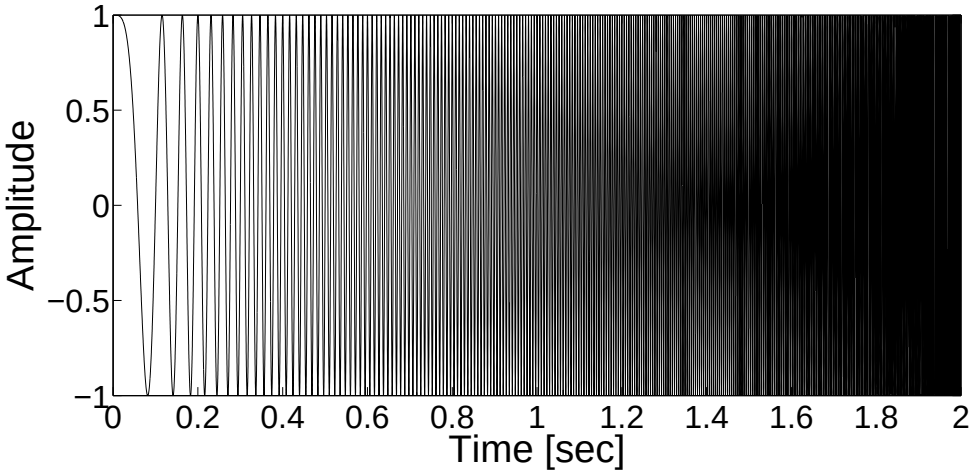


Figure 1: Chirp signal, time domain.

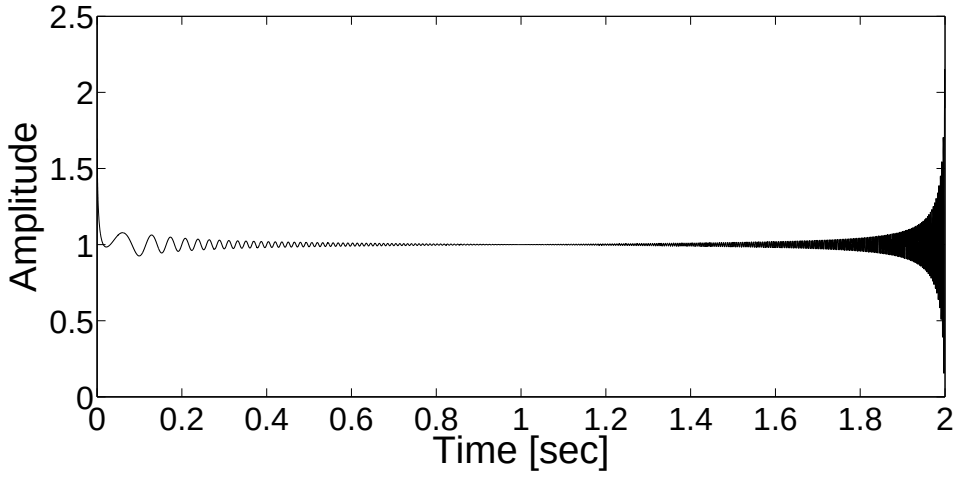


Figure 2: Amplitude envelope using the Hilbert Transform

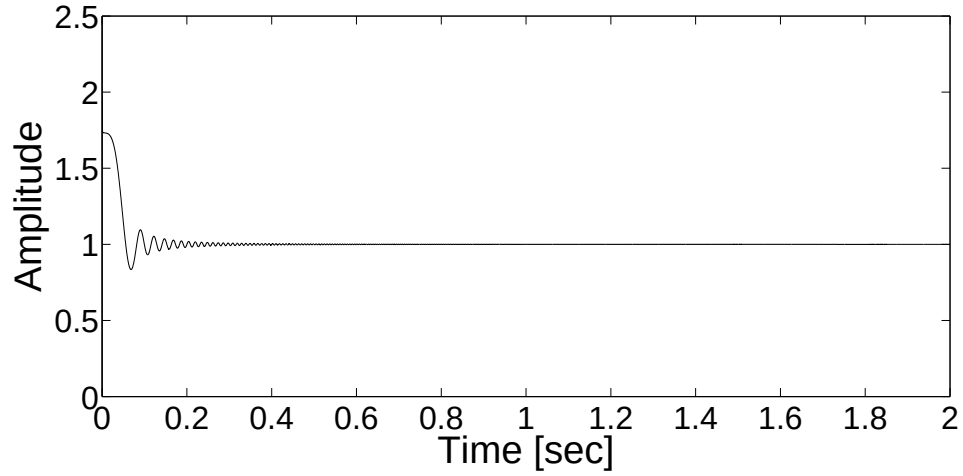


Figure 3: Amplitude envelope using the Teager method.

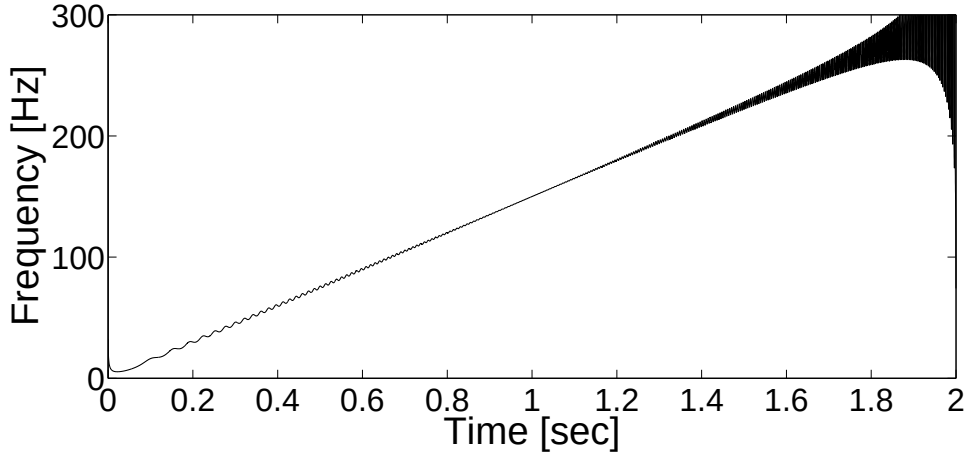


Figure 4: Instantaneous frequency using the Hilbert Transform.

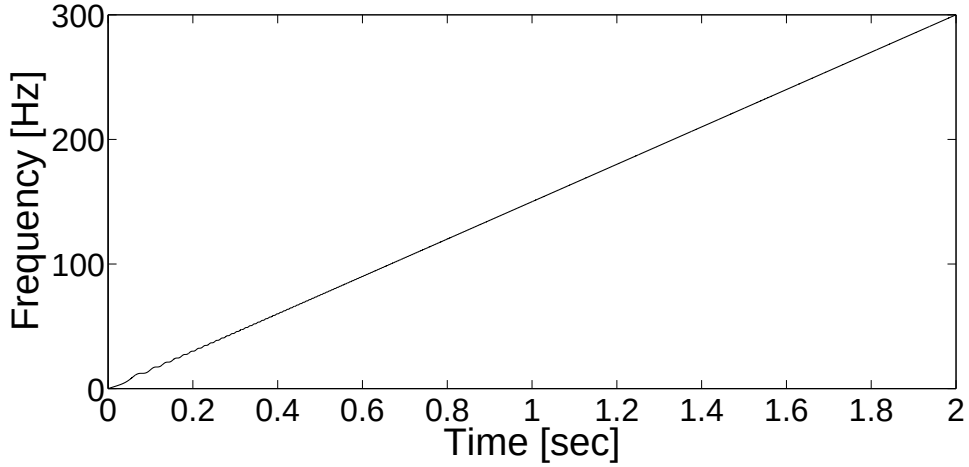


Figure 5: Instantaneous frequency using the Teager method

# 7 Experimental data description

The gearbox vibration data analysed in this study come from an NEG Micon NM $1000/60$ wind turbine in Poland. The gearbox is described by the following kinematic scheme:

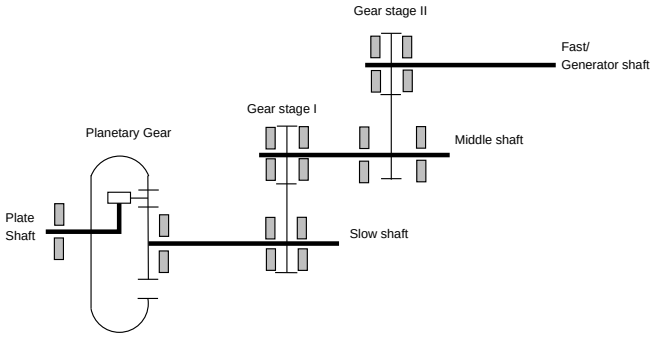


Figure 6: Kinematic scheme of the wind turbine gearbox examined

Acceleration signals from this gearbox were obtained on three different dates: 31/10/2009, 11/2/2010 and 4/4/2010. The first dataset was described as the one to be used as a reference, meaning that no damage was identified up to that date. The second dataset was considered to be the one describing an early damage of the gearbox and the third one was the dataset of the vibration signal with confirmed tooth loss in the gearbox.

When a gearbox has two or more mesh stages, signal processing of its vibration signals becomes more challenging because there are multiple shaft speeds and meshing frequencies apart from noise. This means, for the case of gear tooth damage, that one should examine the specific frequencies associated with the meshing frequencies of the damaged gears. Figure 7 shows 12300 points of the time domain signal of the dataset obtained on 31/10/2009. The gearbox examined has a 28-tooth gear (smaller wheel) rotating at $1500$ rpm that meshes with an 86-tooth gear (bigger wheel) at the parallel gear stage II. The parallel gear stage II is the one at which damage was observed. The rotating frequency of the smaller wheel gear is therefore, $(28/86) * 1500 = 488,372$ rpm $= 8.139$ Hz. Now concerning the frequency spectrum of the signal shown in Figure $8$, noise has been removed, using a low-pass filter, and the frequency components (meshing frequencies and their harmonics) are the following:

- $2.3$ Hz: relative meshing frequency of the planetary gear,
- $14.3$ Hz: relative meshing frequency of the $1^{st}$ gear stage,
- $28, 56, 112, 168, 224$ Hz: relative meshing frequency of the $2^{nd}$ gear stage.

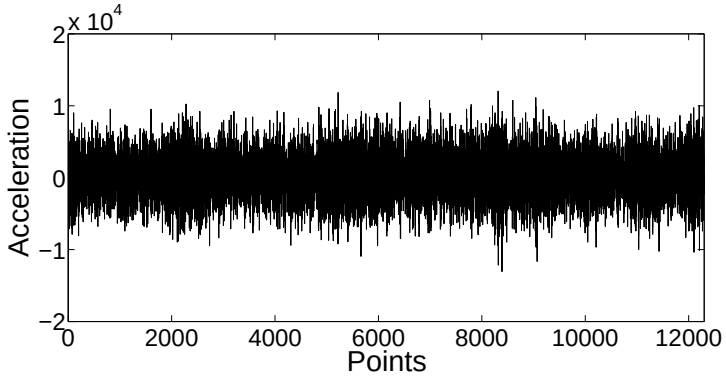


Figure 7: Time history of the gearbox vibration signal at the first state examined (31/10/2009).

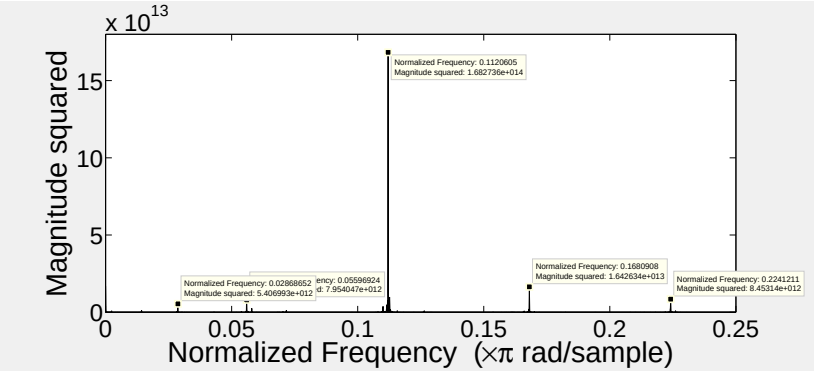


Figure 8: Frequency spectrum of the signal shown in Figure 7.

# 8 Results and discussion

## 8.1 The signal decomposition

Figures 9, 10 and 11, display the results of the EMD. The diagrams represent four gear revolutions. Only the first five intrinsic mode functions of each signal are presented, because they are the ones that contain the highest signal frequencies, therefore, they are more suitable for damage identification. More particularly, the first IMF is related to the noise of the signal, the second to part of the second harmonic of the meshing frequency of the parallel gear stage II, the third to a second part of the same harmonic, the fourth to the meshing frequency of the same stage and the rest of the IMFs to meshing frequencies and harmonics of the other two stages (lower frequencies).

The tooth fault is depicted in the second IMF (Figures 9, 10 and 11), taking the form of periodic pulses with the period of the pinion revolution. The analysis presented in the figures, shows that the $2^{nd}$ and $3^{rd}$ IMFs are sensitive to the damage severity level. Moreover, the instantaneous amplitude of the $2^{nd}$ IMF seems to be the one more sensitive to the evolution of damage, as shown in [25].

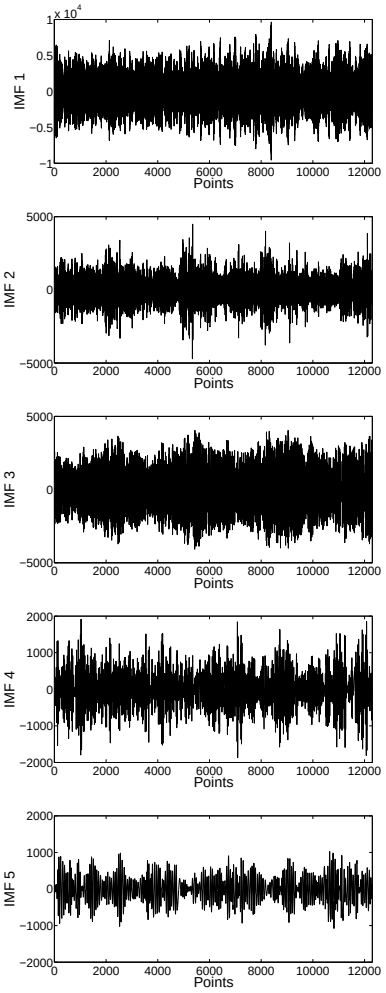


Figure 9: IMFs (31/10/2009).

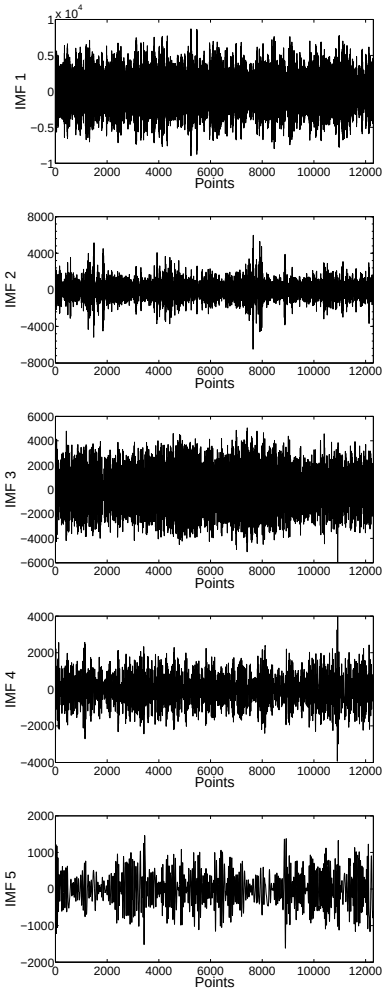


Figure 10: IMFs (11/2/2010).

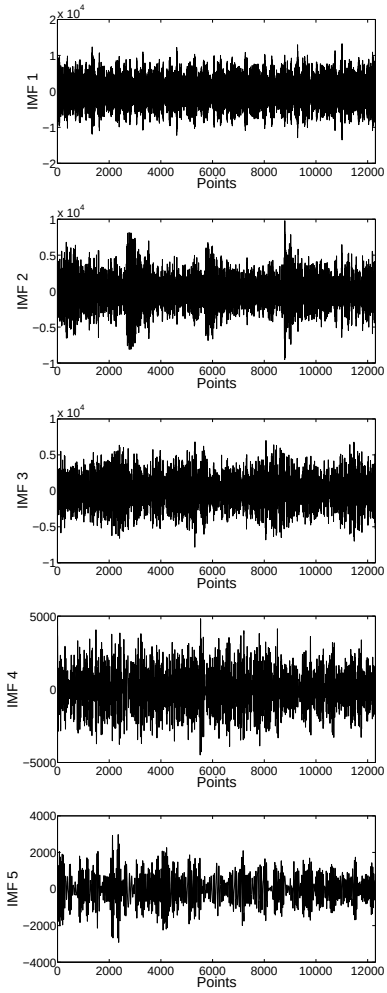


Figure 11: IMFs (4/4/2010).

## 8.2 The Hilbert Transform results

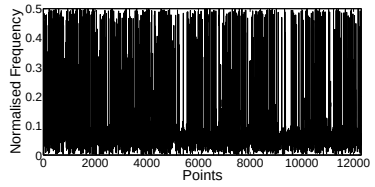


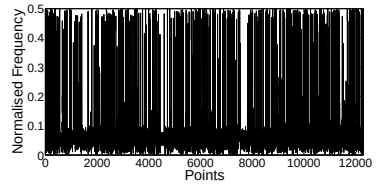


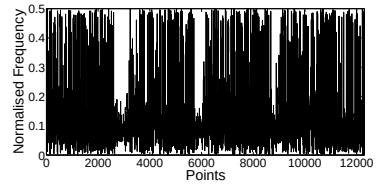


Figure 12: Inst. Frequency of the sum of the $2^{nd}$ and $3^{rd}$ IMFs (31/10/2009, 11/2/2010, and 4/4/2010 datasets).

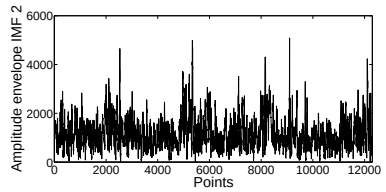


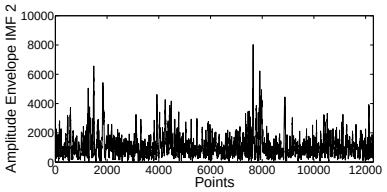


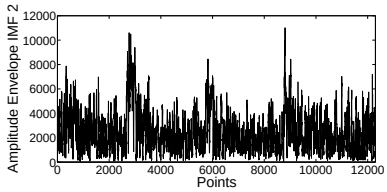


Figure 13: Envelope amplitude of the $2^{nd}$ IMF (31/10/2009, 11/2/2010, and 4/4/2010 datasets).

The presence of damage results in a sudden increase of the vibration energy described by the specific mode. If one keeps in mind the fact that the energy of a signal is proportional to the signal's amplitude, one can assume that the presence of damage can be shown in the amplitude envelope diagrams as an increase of the amplitude at the specific points where damage occurs. This is confirmed in Figure 13. In addition, frequency is lowered at the points where damage occurs (Figure 12), and at the same point at the IMF diagrams damage is shown in the signals as impulses. The author believes that the first data set (31/10/2009) shows some presence of damage at its early stage, since the energy levels of the fault are significantly lower, something that is concluded by taking into consideration the combined results of the $2^{nd}$ IMF's diagram and the diagrams of its amplitude envelope and instantaneous frequency.

The instantaneous frequency diagrams of the sum of the $2^{nd}$ and $3^{rd}$ IMFs, (Figure 12), show that frequency is lowered in this case in some periods of the gear rotation, something that confirms this speculation. The fact that there wasn't recognised any damage at that date by the condition monitoring systems of the specific gearbox, probably using conventional signal processing techniques such as Fourier Transform, proves that the EMD method improves the analysis.

## 8.3 The TKEO (DESA-2) results

The TKEO is a computationally simple algorithm, temporally localised and capable under appropriate signal constraints of accurately tracking the instantaneous amplitude and instantaneous frequency of the signal [23]. In addition, DESA-2 offers low computational complexity and for constant amplitude and linear phase of the signal there are no approximation errors.

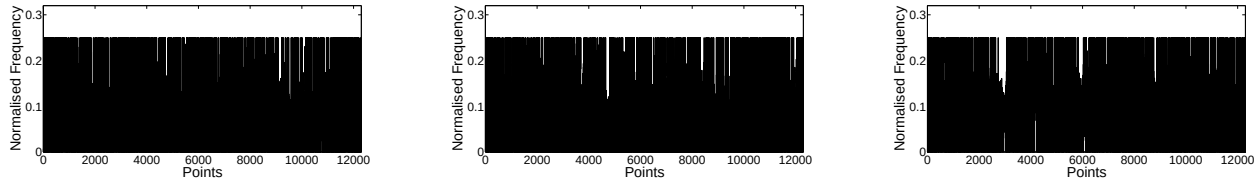


Figure 14: Inst. Frequency of the $2^{nd}$ and $3^{rd}$ IMFs using TKEO (31/10/2009, 11/2/2010, and 4/4/2010 datasets)

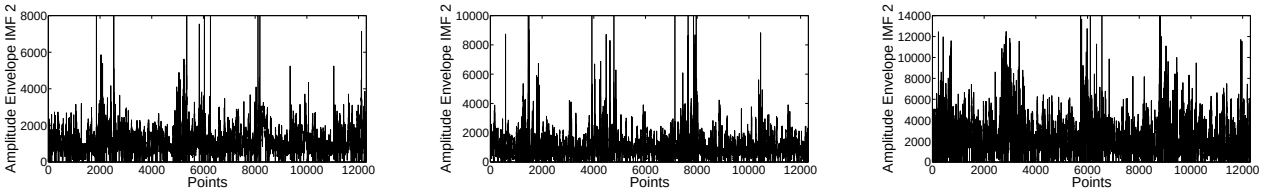


Figure 15: Envelope amplitude of the $2^{nd}$ IMF using TKEO (31/10/2009, 11/2/2010, and 4/4/2010 datasets)

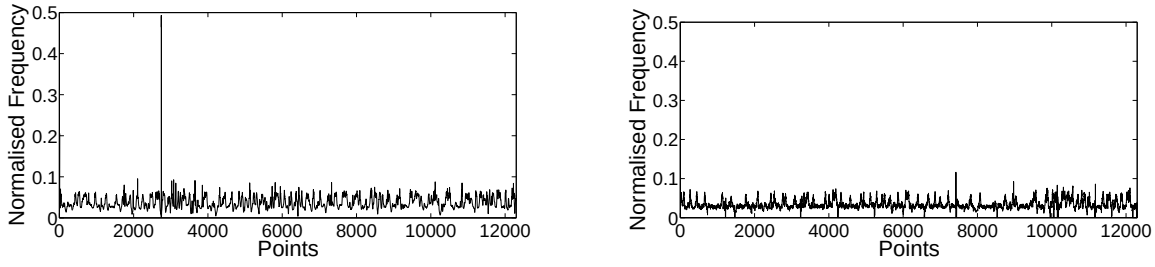


Figure 16: The instantaneous frequency diagrams of the $4th$ IMF, data set (11/2/2010). The $1^{st}$ diagram is obtained using the Hilbert Transform and the $2^{nd}$ using the TKEO and DESA-2.

As mentioned in a previous section,the DESA-2 algorithm can only reach frequencies upto $1/4$ of the sampling frequency of the data, which is a disadvantage of the method. In the particular case of the gearbox data examined, the sampling frequency of $25$ KHz proved a little too low for the estimation of the frequency bandwidths of the data that were most sensitive to damage, as shown in Figure $24$. For this reason, the instantaneous frequencies of the sum of the $1^{rst}$ and $2^{nd}$ IMFs can only be estimated using the Hilbert Transform, and one could use only these results for feature selection (Figure 22). On the other hand, the lower frequencies of the data were estimated with at least the same resolution, if not better, than that offered by the Hilbert Transform (Figure 26). Keeping in mind that previous work by the author showed that the feature most sensitive to damage evolution is the instantaneous amplitude of the highest IMFs ([24, 25]), even if the sampling frequency was satisfactory to estimate the instantaneous frequency of the sum of the $2^{nd}$ and $3^{rd}$ IMFs, in the end the instantaneous amplitude would probably prove to be a better characteristic of the signal for feature selection, ([25]). Examining the instantaneous amplitude results of both methods,as in Figures $25$ and $23$, the TKEO and DESA-2 method seems to be more sensitive to the signal's changes, giving more obvious indicators of presence of damage in the first dataset examined (31/10/2009), although the work done so far is not enough to make definite conclusions.

# 9 Conclusions

The purpose of this work is to use a recent signal processing method for the condition monitoring of a wind turbine gearbox. The TKEO is an energy tracking algorithm, first introduced in speech processing with promising results. Combined with the energy separation algorithm, DESA-2, it can be used to estimate the instantaneous frequency and amplitude envelope of a signal. This is an alternative approach to the approach of the Hilbert Transform, that is why the results obtained by the TKEO in combination with the DESA-2 method are compared to the results given by the Hilbert Transform. The TKEO applies to bandpass signals, so if the signal being examined is a multicomponent signal, bandpass filtering is needed. In this case, the Empirical Mode Decomposition algorithm was used as a filter bank method, and each intrinsic mode function obtained, representing a different bandwidth of frequencies of the signal, was analysed separately with the use of both the Hilbert transform decomposition method and the TKEO in combination with DESA-2. It was shown that the TKEO has the advantages of high resolution and low computational requirements as an algorithm, but it also has the disadvantage of inability to estimate frequencies higher than $1/4$ of the sampling frequency. In the case of the signal processing of the wind turbine gearbox vibration data, the datasets used were taken at sampling frequencies of $25$ kHz which didn't prove to be satisfactorily high enough. The analysis with the Hilbert Transform showed that the modes more dependent to damage were the highest modes of the signal, and more particularly the $2^{nd}$ IMF. Despite the fact that in this particular case, the TKEO failed to estimate specific frequency components of the signal that were important for the condition monitoring of the gearbox, the author believes that the method could be used successfully,with the condition that the measurements should be taken at sampling frequencies that could satisfy the algorithm's needs or by using different approximation methods for estimating the instantaneous frequency, resulting in the appropriate trigonometrical expressions, e.g. methods similar to DESA-1 algorithm. In this case, the TKEO could be a good alternative to other time-frequency methods, offering higher resolution and much lower computational complexity.

# Acknowledgements

This work is part of SYSWIND project, under the Marie Curie Network, and funded by the European Commission Seventh Framework Program.

## References

[1] S.W. Doebling, C.R. Farrar, M.B. Prime, D.W. Shevitz, *Damage and health monitoring of structural and mechanical systems from changes in their vibration characteristics: A literature review*, Los Alamos National Laboratory (1996).

[2] J. Antoni, R. B. Randall, *The spectral kurtosis: application to the vibratory surveillance and diagnostics of rotating machines*, Mechanical Systems and Signal Processing, Vol. 20, No. 2, (2006), pp. 308-331.

[3] M. Inapolat, A. Kahraman, *A theoretical and experimental investigation of modulation sidebands of planetary gear sets*, Journal of Sound and Vibration, Vol. 323, No. 3-5, (2009), pp. 667-696.

[4] M. Inapolat, A. Kahraman, *A dynamic model to predict modulation sidebands of a planetary gear set having manufacturing errors*, Journal of Sound and Vibration, Vol. 329, No. 4, (2010), pp. 371-393.

[5] M. El Badaoui, F. Guillet, J. Danière, *New applications of the real cepstrum to gear signals, including definition of a robust fault indicator*, Mechanical Systems and Signal Processing, Vol. 18, No. 5, (2004), pp. 1031-1046.

[6] W. J. Staszewski, K. Worden and G. R. Tomlinson, *Time-frequency analysis in gearbox fault detection using the Wignar-Ville distribution and pattern recognition*, Mechanical Systems and Signal Processing, Vol. 11, No. 5, (1997), pp. 673-692.

[7] W.J. Staszewski, G.R. Tomlinson, *Application of the wavelet transform to fault detection in a spur gear*, Mechanical Systems and Signal Processing, Vol. 8, No. 3, (1994), pp. 289-307.

[8] J. Antoni, R.B. Randall, *Differential Diagnosis of Gear and Bearing Faults*, Journal of Vibration and Acoustics, Vol. 124, No. 2, ASME (1994), pp. 165-171.

[9] Z.K. Peng, F.L. Chu, *Application of the wavelet transform in machine condition monitoring and fault diagnostics: a review with bibliography*, Mechanical Systems and Signal Processing, Vol. 18, No. 2, (2004), pp. 199-221.

[10] N.E. Huang, Z. Shen, S.R. Long, M.C. Wu, H.H. Shih, Q. Zheng, N. Yen, C. Tung, H.H. Liu, *The empirical mode decomposition and the Hilbert spectrum for nonlinear and non-stationary time series analysis*, Proceedings of the Royal Society of London. Series A: Mathematical, Physical and Engineering Sciences, Vol. 454, No. 1971, (1998), pp. 903-995.

[11] R. Ricci, P. Pennacchi *Diagnostics of gear faults based on EMD and automatic selection of intrinsic mode functions*, Mechanical Systems and Signal Processing, Vol. 25, No. 3, (2011), pp. 821-838.

[12] A. Parey, M. El Badaoui, F. Guillet, N. Tandon, *Dynamic modelling of spur gear pair and application of empirical mode decomposition-based statistical analysis for early detection of localized tooth defect*, Mechanical Systems and Signal Processing, Vol. 294, No. 3, (2006), pp. 547-561.

[13] H.M. Teager, S.M. Teager, *A phenomenological model for vowel production in the vocal tract*, ch. 3, pp. 73-109. San Diego, CA: College-Hill Press, (1985).

[14] H.M. Teager, S.M. Teager, *Evidence for Nonlinear Sound Production Mechanisms in the Vocal Tract*, 55 of D, pp. 241-261. France: Kluwer Academic Publications, (1990).

[15] J.F. Kaiser, *On a simple algorithm to calculate the 'energy' of a signal*, International Conference on Acoustics, Speech, and Signal Processing, (1990),Vol. 1, pp. 381-384.

[16] J.F. Kaiser, *On Teager's energy algorithm and its generalization to continuous signals*, Proceedings of IEEE DSP Workshop, (1990)

[17] D. Gabor, *Theory of communication*, Journal Institution of Electrical Engineers London, Vol. 93, No. 3, (1946), pp. 429-457.

[18] D. Vakman, *On the analytic signal, the Teager-Kaiser energy algorithm, and other methods for defining amplitude and frequency*, IEEE Transactions on Signal Processing, Vol. 44, No. 4, (1996), pp. 791-797.

[19] E. Kvedalen, *Signal processing using the Teager energy operator and other nonlinear operators*, PhD thesis, (2003), Department of Informatics, University of Oslo

[20] P. Maragos, J.F. Kaiser, T.F. Quartieri, *Energy separation in signal modulations with application to speech analysis*, IEEE Transactions on Signal Processing, Vol. 41, No. 10, (1993), pp. 3024-3051.

[21] A. Potamianos, P. Maragos, *A comparison of the Energy operator and the Hilbert Transform approach to signal and speech demodulation*, Signal Processing, Vol. 37, No. 1, (1994), pp. 95-120.

[22] K. Worden, G. Manson, N.R.J. Fieller, *Damage detection using outlier analysis*, Mechanical Systems and Signal Processing, Vol. 229, No. 3, (2000), pp. 647-667.

[23] M.J. Lipsey, J.P. Havlicek, *On the Teager-Kaiser energy operator "low frequency error"*, The 45th Midwest Symposium on Circuits and Systems, Vol. 3, 2002, pp. 53-56

[24] I. Antoniadou, G. Manson, N. Dervilis, W.J. Staszewski, K. Wordem, *On damage detection in wind turbine gearboxes using Outlier analysis*, Proc. SPIE 8343, 83430N (2012), San Diego, California

[25] I. Antoniadou, G. Manson, N. Dervilis, T. Barszcz, W. Staszewski, K. Worden *Condition monitoring of a wind turbine gearbox using the Empirical Mode Decomposition method and Outlier analysis*, $6^{th}$ European Workshop on Structural Health Monitoring, (2012), Dresden